

Daily and intraseasonal relationships between lightning and NO₂ over the Maritime Continent

Katrina S. Virts,¹ Joel A. Thornton,¹ John M. Wallace,¹ Michael L. Hutchins,² Robert H. Holzworth,² and Abram R. Jacobson²

Received 20 June 2011; revised 26 August 2011; accepted 4 September 2011; published 8 October 2011.

[1] The relationship between lightning and NO₂ over Indonesia is examined on daily and intraseasonal time scales based on lightning observations from the World Wide Lightning Location Network (WWLLN) and tropospheric NO₂ column densities from the Global Ozone Monitoring Experiment (GOME-2) satellite mission. Composites of the daily NO₂ observations regressed onto lightning frequency reveal a plume of enhanced NO₂ following a day of enhanced lightning. Lightning and NO₂ also vary coherently with the intraseasonal Madden-Julian Oscillation (MJO) in a manner distinct from the cloudiness signature, with variations of up to ~50% of the annual mean. **Citation:** Virts, K. S., J. A. Thornton, J. M. Wallace, M. L. Hutchins, R. H. Holzworth, and A. R. Jacobson (2011), Daily and intraseasonal relationships between lightning and NO₂ over the Maritime Continent, *Geophys. Res. Lett.*, 38, L19803, doi:10.1029/2011GL048578.

1. Introduction

[2] Nitrogen oxide radicals (NO_x = NO + NO₂) catalyze the production of ozone, a greenhouse gas, and, by regulating the partitioning of hydrogen oxide radicals, they mediate the troposphere's oxidizing capacity [Logan *et al.*, 1981; Mickley *et al.*, 1999; Shindell *et al.*, 2009]. Lightning is an important but uncertain natural source of NO_x, estimated to be on the order of 1–10 Tg N yr⁻¹ globally [Schumann and Huntrieser, 2007; see also Boersma *et al.*, 2005; Lamarque *et al.*, 1996; Martin *et al.*, 2007; Bucseles *et al.*, 2010], or about 5–10% of the present-day global tropospheric NO_x source [Jaegle *et al.*, 2005], and is thought to be responsible for 20–45% of tropical upper tropospheric ozone [e.g., Labrador *et al.*, 2005; Grewe, 2007]. Existing uncertainties in the lightning NO_x source limit our ability to assess the degree to which the atmosphere's energy balance and oxidizing capacity have been perturbed by human activities [Mickley *et al.*, 2001; Wang and Jacob, 1998].

[3] The lightning NO_x source remains uncertain for many reasons, including the physics and detection of lightning itself and the difficulty in detecting lightning NO_x and distinguishing it from other NO_x sources, such as surface combustion [e.g., Beirle *et al.*, 2010]. Here we provide a unique observational analysis of the relationship between tropospheric NO₂ vertical column density and lightning frequency

near Indonesia based on regression analysis performed on daily data and composite maps for various phases of the Madden-Julian Oscillation (MJO).

2. Data

[4] Based on an analysis of data from the SCIAMACHY satellite by Beirle *et al.* [2010], we expect the correlation between the frequency of lightning strokes and NO₂ to be weak, requiring a large sample size to detect a statistically significant signal. Accordingly, we chose to utilize data from the Global Ozone Monitoring Experiment (GOME-2) with its larger areal coverage, which enables us to sample the NO₂ response to 4–5 times as many lightning strokes as would be possible using SCIAMACHY data (see Section 1 of Text S1 in the auxiliary material for a discussion of the statistical significance of our results).¹

[5] The GOME-2 scanning spectrometer provides slant-path, total NO₂ retrievals, from which tropospheric NO₂ vertical column densities, hereafter referred to as NO₂ columns or simply as NO₂, are extracted [Boersma *et al.*, 2004]. The Fast Retrieval Scheme for Clouds from the Oxygen A band (FRESCO) algorithm derives radiance-based effective cloud fractions from GOME-2 retrievals, and a different algorithm indicates whether the tropospheric NO₂ retrieval was meaningful [Koelemeijer *et al.*, 2001]. The collocation of FRESCO cloud fraction with GOME-2 NO₂ observations allows testing for the effects of cloud contamination.

[6] The World Wide Lightning Location Network (WWLLN) is a network of 54 detector stations that monitor very low frequency radio waves called lightning sferics. The time of group arrival of the radiated waveform is used to locate lightning to within ~5 km. The average detection frequency for all lightning strokes over Indonesia during the period of overlap with GOME-2 can be represented to first order as ~10% [Rodger *et al.*, 2009] (see also Section 2 of Text S1). Of the detected WWLLN strokes the median stroke power in the area of this study was $2 \cdot 10^6$ W at the end of 2009 [Hutchins *et al.*, 2010], which is low enough that nearly all lightning-producing storms are detected [Jacobson *et al.*, 2006].

[7] The NO₂ and lightning datasets were gridded and averaged as follows. GOME-2 tropospheric NO₂ retrievals flagged as not meaningful by the GOME-2 quality control algorithms were discarded, and the remaining data from April 2007 to October 2010 were averaged onto a daily 1° latitude × 1° longitude grid; similar averaging was performed for FRESCO cloud fractions. GOME-2 overpasses are at 9:30 LT; i.e., at 0130 UTC over the western part of our domain and

¹Department of Atmospheric Sciences, University of Washington, Seattle, Washington, USA.

²Department of Earth and Space Sciences, University of Washington, Seattle, Washington, USA.

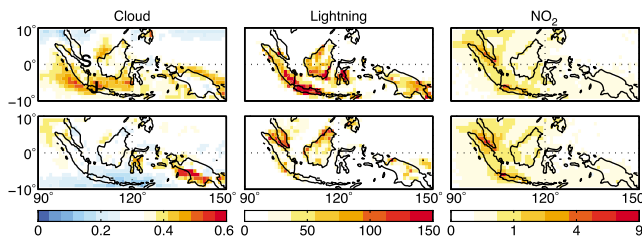


Figure 1. (left) Mean cloud fraction, (middle) lightning frequency (strokes day⁻¹ deg⁻²), and (right) tropospheric NO₂ column (10¹⁵ molecules cm⁻²) during (top) December–February (DJF) and (bottom) June–August (JJA). Lightning color bar is limited to lower values. In upper left panel, S and J indicate locations of Singapore and Jakarta, respectively.

2330 UTC of the previous day in the eastern part of our domain (10°S to 10°N; 90°E to 150°E). WLLN strokes were counted daily (from 0200 UTC to 0159 UTC so that each “day” ends at approximately the time of the GOME-2 overpass) in each 1° × 1° bin of the study area for January 2005 to October 2010. An 80-day high-pass Lanczos filter was applied to the daily time series of each variable, as indicated, to remove the poorly sampled low frequency variability.

[8] In section 4, the Madden-Julian Oscillation is represented by the daily Real-Time Multivariate MJO index developed by *Wheeler and Hendon* [2004], which is based on the dominant modes of variability in near-equatorial outgoing longwave radiation (OLR, a measure of the prevalence of clouds with high, cold tops) and zonal winds in the lower (850 hPa) and upper (200 hPa) troposphere.

3. Seasonal Mean and Daily Variability

[9] Seasonal-mean cloud fraction, lightning frequency, and tropospheric NO₂ column over the Maritime Continent are shown in Figure 1. Lightning tends to be more frequent in the summer hemisphere, with maxima along the coasts of the larger islands. In contrast, the NO₂ seasonal cycle is anchored to sources such as urban areas and ship tracks (e.g., extending west from the northern tip of Sumatra during DJF [*Richter et al.*, 2004]).

[10] Coupled day-to-day variability in lightning and NO₂ is revealed by lag-regression analysis of daily, 80-day high-pass filtered data. The 100 1° × 1° grid boxes with the highest annual-mean lightning frequency are designated as “reference grid boxes;” most are over land, but similar results are obtained using ocean reference boxes (see Section 3 of Text S1). NO₂ time series for each grid point within a 20° × 20° box centered on the reference grid point are regressed onto time series of lightning at the reference grid point summed over the 24 hours before and after the GOME-2 overpasses. The 100 regression maps for NO₂ observations prior and subsequent to the lightning observations are then centered on their respective reference grid boxes and averaged to form the composite lag regression maps shown in Figure 2.

[11] NO₂ observations subsequent to days of enhanced lightning reveal enhanced NO₂ around the reference point. The westward shift of the NO₂ feature relative to the reference grid box likely reflects advection by winds in the middle and upper troposphere, which have an easterly component during all months. The weaker NO₂ maximum near the reference grid box on the day prior to the lightning observations is

likely due to day-to-day autocorrelation of both lightning frequency and NO₂. Similar patterns are obtained when the analysis is performed with NO₂ observations for which the FRESKO cloud fraction was <0.1 (see Section 3 of Text S1). Hence, cloud contamination does not appear to be a significant issue.

[12] An accurate determination of the average impact of a single lightning stroke on NO_x in the surrounding region requires a detailed accounting of the WLLN detection efficiency, systematic uncertainties in the NO₂ retrievals, and consideration of NO_x partitioning, chemistry, and transport on the timescale of ~1 day, all of which are beyond the scope of this paper. However, as a check on whether the above results are reasonable, NO₂ production in this region can be roughly estimated from the subsequent regression map. Summing the regression coefficients for both lightning and NO₂ within 5° relative latitude and longitude of the reference boxes and assuming that WLLN detected ~10% of the lightning strokes over Indonesia during the period of overlap with GOME-2, we estimate between 1.7 and 2.5 × 10²⁵ NO₂ molecules are produced per stroke regardless of whether we use all retrievals classed as meaningful in accordance with the FRESKO criterion or whether we sample only retrievals with cloud fractions < 0.1. Our estimates also fall within this range if we sample only reference grid boxes that lie over water. Further specifics of these sensitivity tests are reported in Section 3 of Text S1. If we use results from *Beirle et al.* [2009] for estimating the production of NO_x per lightning stroke (LNO_x) from satellite observations of NO₂, our LNO_x estimates generally lie on the lower end of the range of 0.2 to 4.0 × 10²⁶ molecules per stroke summarized previously [*Schumann and Huntrieser*, 2007, and references therein] and within the range of values reported by *Beirle et al.* [2010] based on an analysis of the WLLN data in conjunction with individual overpasses of the SCIAMACHY instrument. All else the same, these lower LNO_x values would correspond to a global LNO_x source ~1.5 Tg N yr⁻¹ for an average global lightning frequency of 44 s⁻¹ [*Schumann and Huntrieser*, 2007; *Beirle et al.*, 2009].

4. Intraseasonal Variability

[13] The Madden-Julian Oscillation [*Zhang*, 2005] dominates tropical atmospheric variability at intraseasonal time scales (30–90 day periods). Its dominant features are often

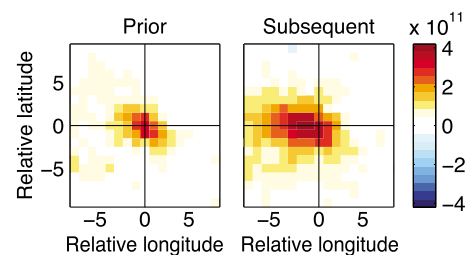


Figure 2. Composites of daily NO₂ field regressed onto daily lightning time series at the 100 grid points with highest lightning frequency (units are molecules cm⁻² stroke⁻¹; both variables have been 80-day high-pass filtered); regressions are performed for NO₂ overpasses prior to and following lightning observations. See text for details.

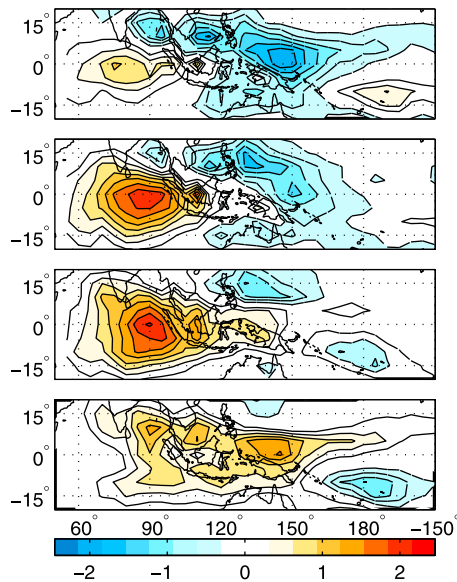


Figure 3. 80-day high-pass filtered 5° latitude × 5° longitude Global Precipitation Climatology Project precipitation (mm day^{-1}) regressed onto time series representing phases 1–4 (top to bottom) of MJO index. Adapted from *Virts and Wallace* [2010].

represented as a cycle made up of eight phases. A characteristic feature of the MJO, shown in Figure 3, is an area of enhanced precipitation that develops over the Indian Ocean during phase 1 and propagates eastward across Indonesia during phases 3 and 4. By construction, the MJO precipitation pattern during the remaining phases (5–8) is identical to those for phases 1–4 but with sign reversed.

[14] MJO cloud, lightning, and NO₂ patterns over Indonesia are shown in Figure 4. The regression coefficient at each grid point has been divided by the annual mean for that point so that, for example, a lightning regression coefficient of 0.5 indicates an MJO perturbation equivalent to 50% of the climatological mean lightning frequency at that point.

[15] In MJO phases 1 and 2, cloudiness is enhanced west of Sumatra and over western Borneo (Figure 4). More extensive clouds are present in phase 3 and cover the marine portion of the domain by phase 4. In association with the enhanced cloudiness, lightning frequency and NO₂ concentrations are also enhanced west of Sumatra and, less prominently, over western Borneo during MJO phase 1. However, lightning and NO₂ both decrease as MJO-related cloudiness and precipitation develop over the study area in MJO phases 2–4. A decrease in lightning during the period of enhanced MJO precipitation has previously been noted in analyses of data from the Tropical Rainfall Measuring Mission [*Morita et al.*, 2006; *Kodama et al.*, 2006]. MJO-induced variations in NO₂ have not, to our knowledge, been discussed, and the patterns in Figure 4 cannot be explained by MJO-related variations in tropopause height (see Section 5 of Text S1). With the exception of western Borneo, the strongest and most coherent MJO cloud, lightning, and NO₂ signals in Figure 4 (and in corresponding correlation maps, see Section 4 of Text S1) are observed over marine areas and not over the areas that exhibit a particularly high annual-mean frequency of occurrence of lightning in Figure 1. The MJO-related variations in NO₂ columns and lightning frequency range up to $\pm 50\%$ of their respective annual mean values.

5. Conclusions

[16] Elevated NO₂ concentrations observed following days of frequent lightning suggest that lightning is an important source of NO_x over Indonesia. The similar evolution of the lightning and NO₂ fields during the MJO offers further confirmation of their covariability. Indeed, it is difficult to imagine how day-to-day changes in surface NO₂ emissions and transport could conspire to create the large scale pattern of NO₂ variability observed in association with the MJO, with perturbations ranging up to 50% of the climatological mean. Such large intraseasonal variability in tropospheric NO_x has implications for oxidants and other trace gases, which could be explored and quantified in conjunction with the methodology used in this paper.

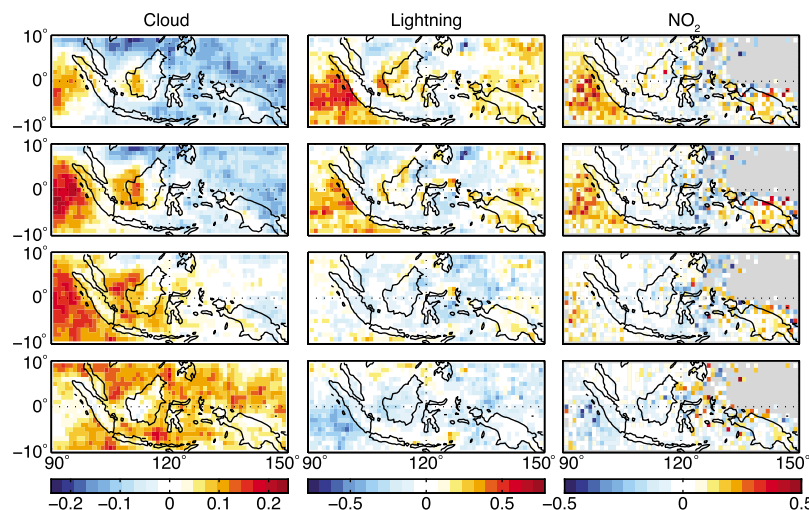


Figure 4. 80-day high-pass filtered (left) cloud fraction, (middle) lightning, and (right) NO₂ regressed onto time series representing MJO phases (top) 1 to (bottom) 4. Regression coefficients are scaled by the annual mean; gray shading indicates areas of low annual mean tropospheric NO₂ column density, where the MJO NO₂ signal is noisy and not statistically significant.

[17] **Acknowledgments.** The authors thank Timothy Bertram, Lukas Valin, and two anonymous reviewers for their helpful suggestions. This work was supported by the National Science Foundation under grant ATM 0812802 and CAREER ATM 08-46183. Tropospheric NO₂ column data from the GOME-2 sensor were obtained from www.temis.nl. Lightning location data were provided by WWLLN (<http://wwlln.net>), a collaboration among over 50 universities and institutions.

[18] The Editor thanks two anonymous reviewers for their assistance in evaluating this paper.

References

- Beirle, S., M. Salzmann, M. G. Lawrence, and T. Wagner (2009), Sensitivity of satellite observations for freshly produced lightning NO_x, *Atmos. Chem. Phys.*, *9*, 1077–1094, doi:10.5194/acp-9-1077-2009.
- Beirle, S., H. Huntrieser, and T. Wagner (2010), Direct satellite observation of lightning-produced NO_x, *Atmos. Chem. Phys.*, *10*, 10,965–10,986, doi:10.5194/acp-10-10965-2010.
- Boersma, K. F., H. J. Eskes, and E. J. Brinksma (2004), Error analysis for tropospheric NO₂ retrieval from space, *J. Geophys. Res.*, *109*, D04311, doi:10.1029/2003JD003962.
- Boersma, K. F., H. J. Eskes, E. W. Meijer, and H. M. Kelder (2005), Estimates of lightning NO_x production from GOME satellite observations, *Atmos. Chem. Phys.*, *5*, 2311–2331, doi:10.5194/acp-5-2311-2005.
- Bucsela, E. J., et al. (2010), Lightning-generated NO_x seen by the Ozone Monitoring Instrument during NASA's Tropical Composition, Cloud and Climate Coupling Experiment (TC⁴), *J. Geophys. Res.*, *115*, D00J10, doi:10.1029/2009JD013118.
- Grewe, V. (2007), Impact of climate variability on tropospheric ozone, *Sci. Total Environ.*, *374*, 167–181, doi:10.1016/j.scitotenv.2007.01.032.
- Hutchins, M. L., R. H. Holzworth, C. J. Rodger, J. B. Brundell, S. F. Abarca, K. L. Corbosiero, and D. Vollaro (2010), Global estimates of lightning peak current from the WWLLN, Abstract AE24A-07 presented at 2010 Fall Meeting, AGU, San Francisco, Calif., 13–17 Dec.
- Jacobson, A. R., R. H. Holzworth, J. Harlin, R. L. Dowden, and E. H. Lay (2006), Performance assessment of the World Wide Lightning Location Network (WWLLN), using the Los Alamos Sferic Array (LASA) as ground-truth, *J. Atmos. Oceanic Technol.*, *23*, 1082–1092, doi:10.1175/JTECH1902.1.
- Jaegle, L., L. Steinberger, R. V. Martin, and K. Chance (2005), Global partitioning of NO_x sources using satellite observations: Relative roles of fossil fuel combustion, biomass burning and soil emissions, *Faraday Discuss.*, *130*, 407–423, doi:10.1039/b502128f.
- Kodama, Y.-M., M. Tokuda, and F. Murata (2006), Convective activity over the Indonesian Maritime Continent during CPEA-I as evaluated by lightning activity and Q1 and Q2 profiles, *J. Meteorol. Soc. Jpn.*, *84A*, 133–149, doi:10.2151/jmsj.84A.133.
- Koelemeijer, R. B. A., P. Stammes, J. W. Hovenier, and J. F. de Haan (2001), A fast method for retrieval of cloud parameters using oxygen A band measurements from the Global Ozone Monitoring Experiment, *J. Geophys. Res.*, *106*, 3475–3490, doi:10.1029/2000JD900657.
- Labrador, L. J., R. von Kuhlmann, and M. G. Lawrence (2005), The effects of lightning-produced NO_x and its vertical distribution on atmospheric chemistry: Sensitivity simulations with MATCH-MPIC, *Atmos. Chem. Phys.*, *5*, 1815–1834, doi:10.5194/acp-5-1815-2005.
- Lamarque, J. F., G. P. Brasseur, P. G. Hess, and J. F. Muller (1996), Three-dimensional study of the relative contributions of the different nitrogen sources in the troposphere, *J. Geophys. Res.*, *101*, 22,955–22,968, doi:10.1029/96JD02160.
- Logan, J. A., M. J. Prather, S. C. Wofsy, and M. B. McElroy (1981), Tropospheric chemistry: A global perspective, *J. Geophys. Res.*, *86*, 7210–7254, doi:10.1029/JC086iC08p07210.
- Martin, R. V., B. Sauvage, I. Folkins, C. E. Sioris, C. Boone, P. Bernath, and J. Ziemke (2007), Space-based constraints on the production of nitric oxide by lightning, *J. Geophys. Res.*, *112*, D09309, doi:10.1029/2006JD007831.
- Mickley, L. J., P. P. Murti, D. J. Jacob, J. A. Logan, D. M. Koch, and D. Rind (1999), Radiative forcing from tropospheric ozone calculated with a unified chemistry-climate model, *J. Geophys. Res.*, *104*, 30,153–30,172, doi:10.1029/1999JD900439.
- Mickley, L. J., D. J. Jacob, and D. Rind (2001), Uncertainty in preindustrial abundance of tropospheric ozone: Implications for radiative forcing calculations, *J. Geophys. Res.*, *106*, 3389–3399, doi:10.1029/2000JD900594.
- Morita, J., Y. N. Takayabu, S. Shige, and Y. Kodama (2006), Analysis of rainfall characteristics of the Madden-Julian Oscillation using TRMM satellite data, *Dyn. Atmos. Oceans*, *42*, 107–126, doi:10.1016/j.dynatmoce.2006.02.002.
- Richter, A., V. Eyring, J. P. Burrows, H. Bovermann, A. Lauer, B. Sierk, and P. J. Crutzen (2004), Satellite measurements of NO₂ from international shipping emissions, *Geophys. Res. Lett.*, *31*, L23110, doi:10.1029/2004GL020822.
- Rodger, C. J., J. B. Brundell, R. H. Holzworth, and E. H. Lay (2009), Growing detection efficiency of the World Wide Lightning Location Network, *AIP Conf. Proc.*, *1118*, 15–20, doi:10.1063/1.3137706.
- Schumann, U., and H. Huntrieser (2007), The global lightning-induced nitrogen oxides source, *Atmos. Chem. Phys.*, *7*, 3823–3907, doi:10.5194/acp-7-3823-2007.
- Shindell, D. T., G. Faluvegi, D. M. Koch, G. A. Schmidt, N. Unger, and S. E. Bauer (2009), Improved attribution of climate forcing to emissions, *Science*, *326*(5953), 716–718, doi:10.1126/science.1174760.
- Virts, K. S., and J. M. Wallace (2010), Annual, interannual, and intraseasonal variability of tropical tropopause transition layer cirrus, *J. Atmos. Sci.*, *67*, 3097–3112, doi:10.1175/2010JAS3413.1.
- Wang, Y. H., and D. J. Jacob (1998), Anthropogenic forcing on tropospheric ozone and OH since preindustrial times, *J. Geophys. Res.*, *103*, 31,123–31,135, doi:10.1029/1998JD100004.
- Wheeler, M. C., and H. H. Hendon (2004), An all-season real-time multivariate MJO index: Development of an index for monitoring and prediction, *Mon. Weather Rev.*, *132*, 1917–1932, doi:10.1175/1520-0493(2004)132<1917:AARMMI>2.0.CO;2.
- Zhang, C. (2005), Madden-Julian Oscillation, *Rev. Geophys.*, *43*, RG2003, doi:10.1029/2004RG000158.

R. H. Holzworth, M. L. Hutchins, and A. R. Jacobson, Department of Earth and Space Sciences, University of Washington, Box 351310, 070 Johnson Hall, Seattle, WA 98195-1310, USA.

J. A. Thornton, K. Virts, and J. M. Wallace, Department of Atmospheric Sciences, University of Washington, Box 351640, 408 ATG Bldg., Seattle, WA 98195-1640, USA. (kvirts@uw.edu)